

# Spatial Variations in Temperature across a Photovoltaic Array

Michaela G. Farr and Joshua S. Stein

Sandia National Laboratory, Albuquerque, NM, 87185, United States

**ABSTRACT** — The efficiency of any photovoltaic device is significantly affected by its operating temperature. It is therefore of great interest to the PV industry to have accurate models of module and array temperatures. Existing PV performance models generally assume that module temperature is a function of plane-of-array irradiance, ambient air temperature and wind speed AND that module temperatures across the array do not vary significantly enough to define. A comparison of two identical PV systems in different climates reveals that module temperatures across the array may in fact vary by several degrees based on the location relative to one another. This study describes the observed thermal patterns and evaluates the possible causes of these systematic variations. The following paper will present analysis of data gathered from two PV systems with identical setups located in Albuquerque NM and Orlando, Florida.

**Index Terms** — Photovoltaics, Cooling, Efficiency, Wind Speed.

## I. INTRODUCTION

The performance of a photovoltaic (PV) system is primarily affected by the irradiance and temperature of the array. The temperature of the array is generally assumed to be a function of irradiance, ambient temperature, and wind speed. For example the Sandia Photovoltaic Array Performance Model (SAPM) [1] assumes the following equation for prediction of the back of module temperature

$$T_m = E * \{e^{a+b*WS}\} + T_a \quad (1)$$

where:

$T_m$  = Back-surface module temperature, (°C).

$T_a$  = Ambient air temperature, (°C)

$E$  = Solar irradiance incident on module surface, (W/m<sup>2</sup>)  
 $WS$  = Wind speed measured at standard 3-m height, (m/s)  
 $a$  = Empirically-determined coefficient establishing the upper limit for module temperature at low wind speeds and high solar irradiance

$b$  = Empirically-determined coefficient establishing the rate at which module temperature drops as wind speed increases

Use of this model to predict temperature implicitly assumes that the entire array is at a uniform temperature. In reality, there may be temperature variations across the array, which may be caused by a number of factors, including: complex wind flow patterns near the array that affects the uniform heat transfer to the environment, uneven soiling, deviations in module efficiency, and even module hotspots from local

shunting or other failures. Since module temperature almost exclusively affects the DC voltage of the operating array and modules are typically connected in series to form strings that in turn are connected in parallel to build arrays, the effect of non-uniform temperatures across the array is likely to affect performance predictions. In this study, we present a new detailed dataset describing observed spatial patterns of module temperatures across two identical arrays in different climates. We evaluated wind speed and wind direction as possible culprits for these temperature discrepancies while eliminating other biasing factors.

## II. METHODS

In this study we instrumented two identical PV arrays (one in Albuquerque, NM and the other near Orlando, FL) with 16 thermocouples attached to the back of CIGS, glass-glass modules distributed in the array as shown in figure 1. Thermocouples were installed on 16 modules in a checkerboard configuration on an array containing 2 racks with 3 rows of 10 modules each. Each rack contains 5 electrical strings, which contain one or two thermocouples as shown:

16		15				11		
			14			12		9
				13			10	

		6				2		1
8			5			3		
	7				4			

Figure 1 - Position of back of module thermocouples



Figure 2 – Sandia National Laboratories Heliovolta Array

We gathered data about wind speed, wind direction, global horizontal irradiance, direct normal irradiance, diffuse horizontal irradiance, and ambient air temperature for each array per second. We evaluated temperature data at each site for several consecutive clear sky days, thereby reducing noise caused by irregular irradiance from passing clouds. We then proceeded to systematically eliminate several sources of temperature error, beginning with calibration error.

Each module data set was corrected by a night time normalization factor to help eliminate systematic calibration error. The night time factor was derived by taking a temperature average of all the thermocouples per array per time step and then subtracting this from each individual module average temperature to find the temperature difference between the two. Module temperatures for each time-step of all four days were corrected up or down by their respective temperature difference from the average. This created a consistent baseline for all the modules

We then plotted temperature vs. time data for each array and found some interesting temperature discrepancies, namely that temperature for both sites generally decreases from North to South. Figure 3 shows an overlay of temperatures for each array for several consecutive clear sky days (9/23-9/26/2013) at the SNL site. The North-most thermocouple is indicated by red and the South-most (right) by blue. All intermediate modules are indicated by black. Note that the areas of little temperature difference occur between sunset and sunrise, which corresponds to zero energy input.

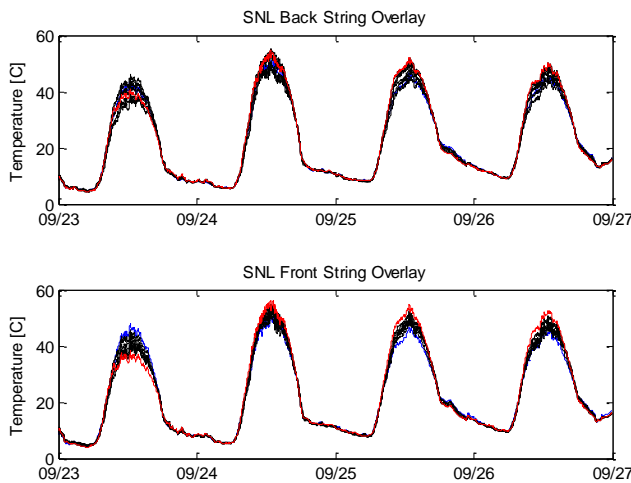


Figure 3 – SNL Module Temperatures

In Figure 3 it can be seen that temperature may vary significantly during the middle of the day with temperature extremes at the north and south ends. Figure 4 helps illustrate this temperature error. Blue represents the difference between north most and south most thermocouples for each array and we can see that the discrepancy may be as much as 10 degrees.

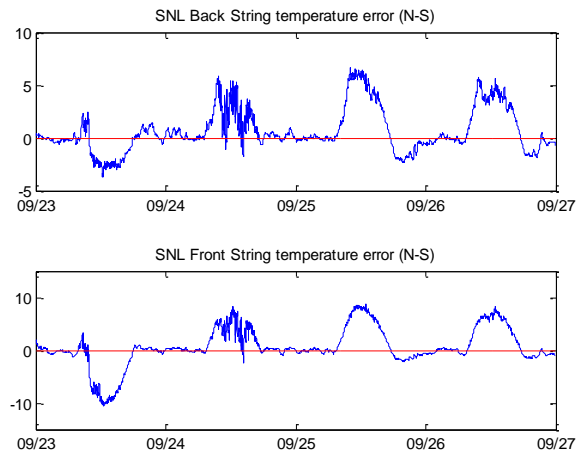


Figure 4 – Temperature Differences between Sides

Data from the FSEC site over four clear sky days (10/25/13-10/28/13) exhibited very similar trends. Like the Sandia array, there may be a large temperature gradient of up to 10 degrees between North and South-most modules, as demonstrated in Figure 5.

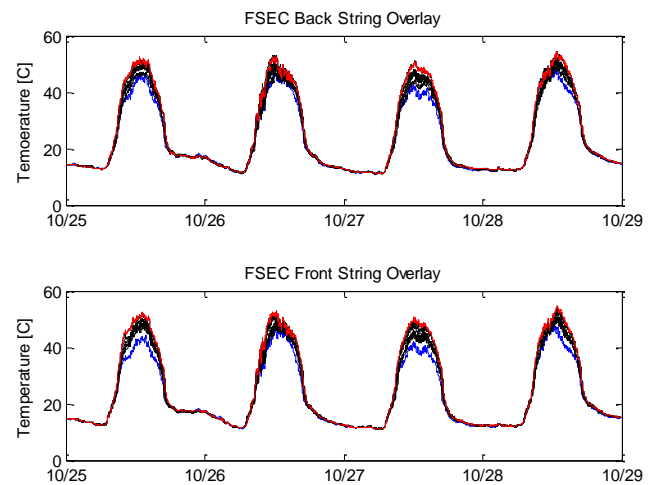


Figure 5 – FSEC Module Temperatures

For the FSEC site the direction of temperature gradient was positive for all four days. Aside from the first day, the SNL site also showed a general tendency for the north-most module to be warmer and the south-most to be cooler. This flip-flop at the beginning seemed to be indicative that wind could be a culprit. If there was an unusual wind direction or speed on that day, it could potentially reverse the direction of a boundary layer on the array's surface.

### III. RESULTS

The following four plots show wind data for each day that was evaluated from the SNL site. The left plots show wind bearing as an angle theta where north is 90 and west is 180. The module is oriented along the y-axis from 270 to 90 deg. Wind speed is represented by magnitude. Red corresponds to times when the temperature difference is greater than or equal to 5 degrees and blue represents when it is less than 5 degrees difference. The right plot shows wind speed as a function of time of day with the colors again corresponding to temperature differences.

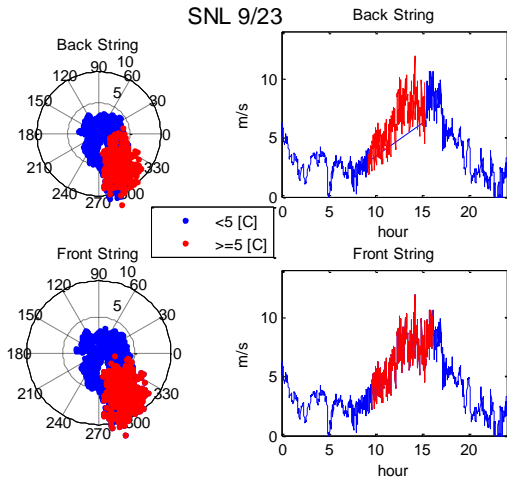


Figure 6 – SNL 9/23 Wind rose

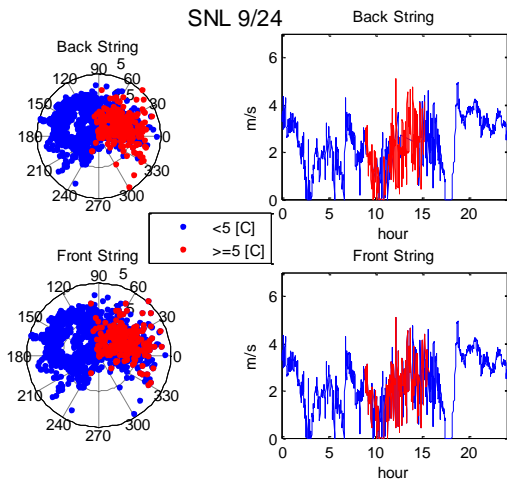


Figure 7 – SNL 9/24 Wind rose

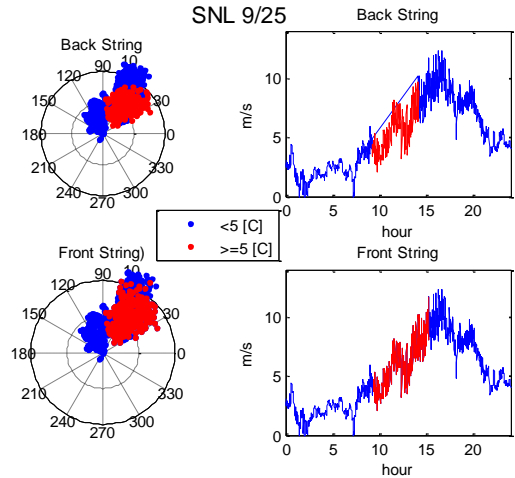


Figure 8 – SNL 9/25 Wind rose

From Figures 6 & 8 we might conclude that lateral winds (north to south or south to north) cause temperature gradients. This trend could perhaps be explained by some sort of boundary layer phenomenon. Yet Figure 7 shows that high temperature gradients can also occur during lateral winds (east to west). The FSEC figures also show that the greatest temperature gradients occur during peak power input. Other days from the FSEC site were examined but were found to be generally uniform in wind speed and direction.

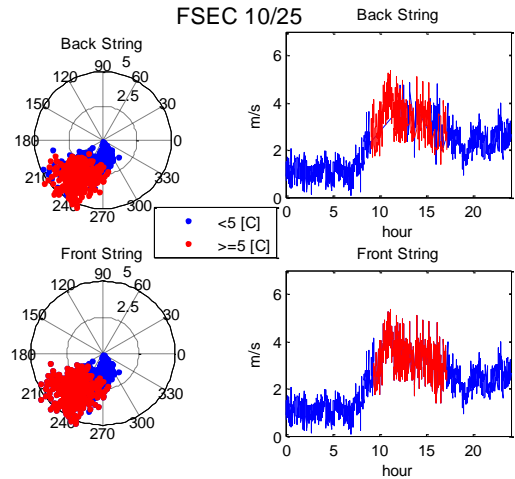


Figure 9 – FSEC 10/25 Wind rose

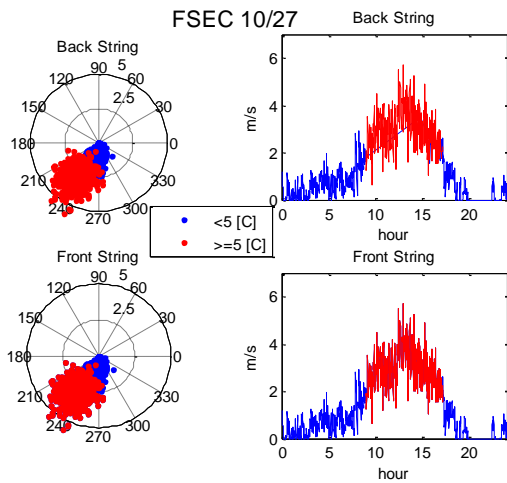


Figure 10 – FSEC 9/27 Wind rose

From the time wind direction/time plots for all three figures we can see that the greatest temperature differences do not occur when wind speed is highest but are concurrent with the time when the array receives the most solar input, between 10:00 am and 3:00 pm. In short, none of these plots prove a definite correlation between temperature gradient and wind velocity or wind direction, at least for those data taken at 10 meters. Either, there is no relationship between the two, or the trends are so local that they do not reflect wind behavior at a slightly higher elevation.

Both data sets seem to show that temperature gradient has a correlation with GHI since both sites exhibited similar behavior regardless of their predominating wind direction. Figures 11 & 12 show each individual module in its respective row for a sample day.

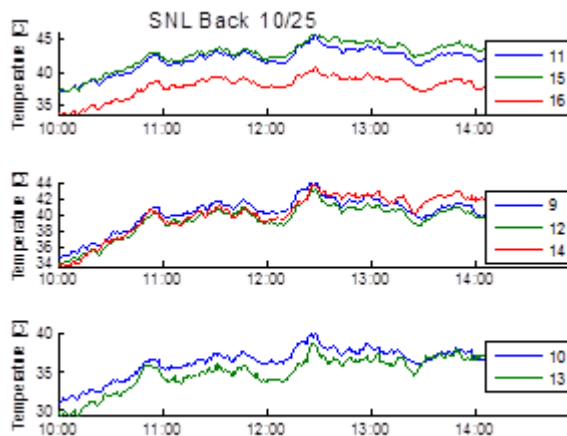


Figure 11 – SNL 10/25 individual modules (back rack)

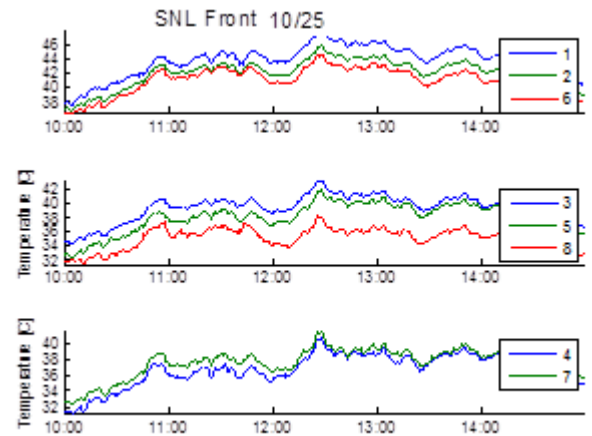


Figure 12 – SNL 10/25 individual modules (front rack)

From the top strings of both front and back arrays it is easy to see temperature variations of up to 5 degrees just within rows. What is especially interesting about these close-ups is that the temperature peaks and valleys move in concert with one another. While module 16 and module 13 are roughly 10 degrees apart they mimic each other in their trends. This is also true between racks. The micro fluctuations shown by 3, 5, and 8 are echoed in 11, 15, and 16. This indicates that temperature differences are not purely a function of North/South location. These harmonized micro-features suggest an electrical issue, as it is hard to imagine that wind forcing could cause such uniform change across an entire array. We then examined individual strings, averaging when there were two thermocouples in a given string. Figures 13, 14 & 15 show the plots of these strings for our sample days at the SNL site. One can also see that strings 4 and 13 are consistently the lowest, while strings 16 and 7/8 are usually the highest. Again, their synchronized micro-fluctuations indicate that there could be some sort of electrical issue at play. Similar trends were found for the FSEC site.

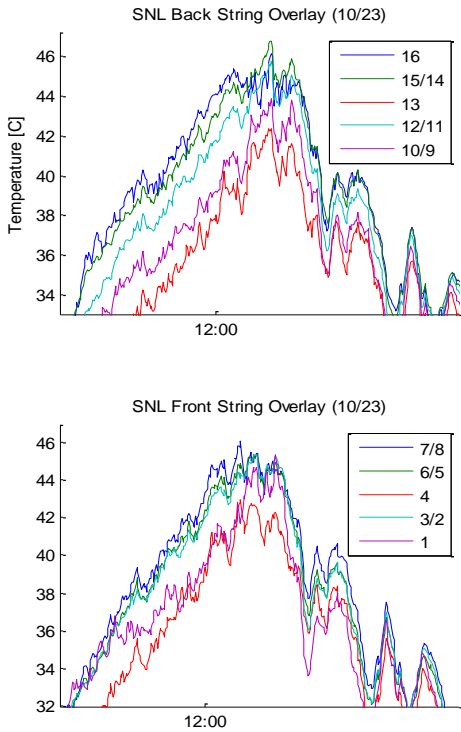


Figure 13 – SNL String Overlay 10/23

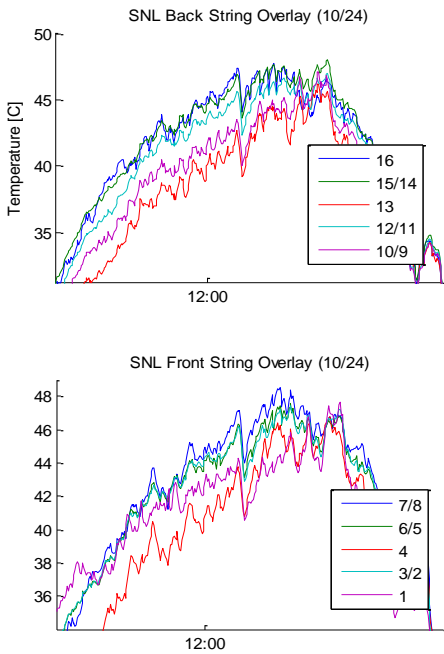


Figure 14 – SNL String Overlay 10/24

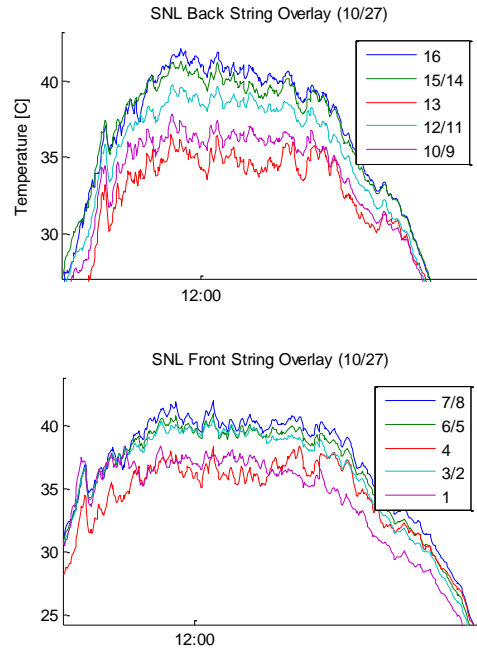


Figure 15 – SNL String Overlay 10/27

One theory was that the length of the runner cable between each string and the power box might cause a drop in voltage significant enough to cause such changes in temperature. To test if the temperature offset was caused by the length of the cable an extra 50 feet of cable was attached to the closest string (string/module 16) thereby equalizing the distance of cable between the closest and furthest string (string/module 9). At this time we would have expected to see a convergence between these two values, yet over the course of 2 weeks no significant difference in the relative rank occurred.

#### IV. CONCLUSIONS

It seems that wind should have a major impact on the temperature of a large surface area which is conducting and convecting heat. Increased fluid flow rate generally correlates to increased uniformity of temperature. But ultimately there does not seem to be a correlation between wind speed and wind direction and temperature gradient. Nor does cable length (and therefore voltage drop) appear to be a culprit. All that can really be concluded is that temperature discrepancies increase with increased GHI, and that there are some sort of systemic phenomena at work that we have yet to fully understand.

#### ACKNOWLEDGEMENT

Sandia is a multi-program laboratory operated by Sandia Corporation, a Lockheed Martin Company, for the United States Department of Energy's National Nuclear Security Administration under contract DE-AC04-94AL85000.

#### REFERENCES

- [1] King, D. L., et al. (2004). Photovoltaic Array Performance Model. Albuquerque, NM, Sandia National Laboratories.
- [2] A. Royne, C. J. Dey, D. R. Mills, et al. (2004). Cooling of Photovoltaic cells under concentrated illumination: a critical review. University of Sydney, Sydney, Australia.

